REPRINTED FROM:

Structural safety

Structural Safety, 12 (1993) 255–276
Elsevier

A benchmark study on importance sampling techniques in structural reliability *

S. Engelund and R. Rackwitz [1]

Technische Universität München, Laboratorium für den Konstruktiven Ingenieurbau, Arcisstr. 21, D-8000 München 2, Germany

ELSEVIER, AMSTERDAM–OXFORD–NEW YORK–TOKYO

Structural Safety, 12 (1993) 255–276
Elsevier

A benchmark study on importance sampling techniques in structural reliability *

S. Engelund and R. Rackwitz [1]

Technische Universität München, Laboratorium für den Konstruktiven Ingenieurbau, Arcisstr. 21, D-8000 München 2, Germany

Abstract. Several widely used importance sampling methods for the estimation of failure probabilities are compared. The methods are briefly reviewed, and a set of evaluation criteria for the comparison of the methods is chosen. In order to perform a fair comparison the developers of the schemes were asked to solve a number of problems selected in view of the evaluation criteria. Their solutions are presented and discussed. Conclusions about the performances of the schemes under different circumstances are given.

Key words: structural reliability; probability integration; Monte Carlo methods; simulation; importance sampling.

1. Introduction

Let $\boldsymbol{X} = (X_1, X_2, \ldots, X_n)$ denote the vector of basic variables of a reliability problem with continuous distribution function $F_{\boldsymbol{X}}(\boldsymbol{x})$ and $g_{ij}(\boldsymbol{X})$ the state function defined in such a way that failure occurs for $\Omega_x = \{\cup \cap g_{ij}(\boldsymbol{x}) \leqslant 0\}$. The failure probability is calculated as:

$$p_f = \int_{\Omega_x} f_{\boldsymbol{X}}(\boldsymbol{x})\, \mathrm{d}\boldsymbol{x} \tag{1a}$$

where $f_{\boldsymbol{X}}(\boldsymbol{x})$ is the joint probability density function of $\boldsymbol{X}$. Alternatively, if a probability distribution transformation $\boldsymbol{X} = \boldsymbol{T}(\boldsymbol{U})$ exists where $\boldsymbol{U}$ is a standard normal independent vector, the failure probability can also be calculated in the so called standard space (u-space). If Ω_{fu} denotes the failure region in the u-space then:

$$p_f = \int_{\Omega_u} \varphi_u(\boldsymbol{u})\, \mathrm{d}\boldsymbol{u} \tag{1b}$$

where φ_u denotes the n-dimensional standard normal density. The necessary probability integration in the u-space can be performed by FORM/SORM [1] which in essence locates

* Discussion is open until May 1994 (please submit your discussion paper to the Editor, Ross B. Corotis).
[1] With contributions from C.G. Bucher, G. Fu, P. Geyskens and J. Johannesen.

numerically the so called most likely failure point (most important region, design point, β-point). In this point the failure boundary is approximated by either a linear or quadratic form whose probability content can be determined analytically. If the distribution function of $\boldsymbol{X}$ is not differentiable and/or the failure domain cannot be represented as before FORM/ SORM concepts are no more suitable for computing the integrals as eqns. (1).

The approximate calculation of failure probabilities of structural components and systems by FORM/SORM is well known. Nevertheless, alternatives for cases where FORM/SORM does not work satisfactorily and methods with which the error by these methods can be quantified are desirable. One of the most attractive alternatives, no doubt, is by applying importance sampling techniques first proposed in 1983 by Shinozuka [2]. Quite a number of variants have been proposed since then each having its merits and disadvantages. A systematic comparison has been missing up to now, except for a study by Fujita and Rackwitz [3] who compared three special schemes. Therefore, the authors decided to arrange a benchmark study. In order to avoid unnecessary bias a number of examples, most of which have been studied previously by one or the other method, were set up covering a large area of applications and the most important judgment criteria. These examples have been recomputed by a part of the developers. Their results form the basis of the comparisons to be made in the following.

2. Evaluation criteria

In order to judge the different importance sampling methods the following quality criteria have been selected.

- Basic variable (x-) or standard (u-) space formulation
- Robustness (against multiple critical points and noisy failure boundaries)
- Capabilities to handle equalities, unions and intersections
- Continuity of limit state function and/or joint distribution function of X
- Efficiency and accuracy (convergence properties) especially with respect to
  - Space dimension
  - Probability level
  - Curvatures of limit state function

There is an ongoing debate about which of the alternative computation schemes in the x- or u-space, respectively, is preferable. The u-space formulations appear to be more widely used at present. They require a probability distribution transformation, which in some cases not only must be performed numerically but also requires some additional programming effort. The transformation can further increase or decrease the nonlinearity of the problem. The same, of course, is true for importance sampling methods. x-space formulations have been put forward in 1978 in the context for FORM (see Rackwitz and Fiessler [4]) and recently in the context of SORM by Breitung [5]. They have been found to work equally well if certain scaling problems can be solved. Importance sampling methods in either space are discussed below.

It is well known that a FORM/SORM analysis can fail when more than one β-point exists. Furthermore, Liu and Der Kiureghian [6] have shown that some of the usual algorithms for FORM/SORM have difficulties in locating the important region when the limit state function contains numerical noise, which may arise from errors in complex state function routines. It is therefore of interest to test whether importance sampling schemes offer an efficient alternative for these special cases.

Most importance sampling schemes have been developed for simple component reliability problems. However, a large number of structural reliability problems involves unions and intersections. Therefore, an important judgment criterion is the capability of a method to handle these problems. The same is true for equalities occurring, for example, in applications when reliabilities are to be updated by observations.

FORM/SORM require the failure function and the distribution functions of the stochastic variables to be continuous. It will be investigated if importance sampling schemes are also limited in this sense.

Taking into account that the evaluation of the failure function usually is the most time-consuming part of the analysis, the efficiency of the methods can be judged by the number of g-function calls which are necessary in order to reach a given coefficient of variation of the failure probability estimate. The number of g-function calls, which are necessary to perform the simulation, includes the calls used to locate the important region and to perform the sampling according the the chosen sampling density.

Structural reliability problems can involve a large number of stochastic variables. In FORM/SORM the numerical effort increases with space dimension. Similarly, the efficiency of various importance sampling schemes depends on the space dimension. Therefore, the dimension of the uncertainty space may also be an important factor in evaluating importance sampling schemes.

Importance sampling methods are used to estimate a wide range of probabilities (typically, 10^{-3}–10^{-10} for structural reliability problems). It is, therefore, important that the efficiency of the methods is insensitive against the probability level.

Finally, because problems with large curvatures of the failure surface in the design point can only be calculated accurately by SORM which can require considerable more effort than FORM it is of special interest to investigate the performance of the importance sampling methods for failure surfaces with extreme curvatures.

3. Importance sampling methods

3.1. Basic concepts

Equation (1) can be written in the following form:

$$p_f = \int_{\Omega_f} \frac{f_X(\boldsymbol{v})}{h_V(\boldsymbol{v})} h_V(\boldsymbol{v})\, \mathrm{d}\boldsymbol{v} = \int_{\mathbb{R}^n} \mathbb{I}[g(\boldsymbol{v}_i) < 0] \frac{f_X(\boldsymbol{v})}{h_V(\boldsymbol{v})} h_V(\boldsymbol{v})\, \mathrm{d}\boldsymbol{v} \tag{2}$$

where $h_V(\boldsymbol{v})$ is the importance sampling density function and $\mathbb{I}[\cdot]$ is the indicator function for Ω_f. If h_V is nonzero over the failure region, an unbiased estimator for p_f is

$$\hat{p}_f = \frac{1}{N} \sum_{i=1}^{N} \mathbb{I}[g(\boldsymbol{v}_i) < 0] \frac{f_X(\boldsymbol{v}_i)}{h_V(\boldsymbol{v}_i)} \approx E(\hat{p}_f) \tag{3}$$

where N outcomes of $\boldsymbol{V}$, $\boldsymbol{v}_i$ are generated from the importance sampling density function h_V. The variance of the estimator for the failure probability is:

$$\mathrm{Var}(\hat{p}_f) = \frac{1}{N-1} \left[\frac{1}{N} \sum_{i=1}^{N} \mathbb{I}[g(\boldsymbol{v}_i) < 0] \frac{f_X(\boldsymbol{v}_i)^2}{h_V(\boldsymbol{v}_i)^2} - \hat{p}_f^2 \right] \tag{4}$$

From eqn. (4) it is clear that the variance of the estimator strongly depends on the importance sampling distribution. The variance reduces to zero if the sampling density is chosen so that it is proportional to $f_X(\boldsymbol{x})$ over the failure region and zero elsewhere. This sampling density, however, depends on the exact solution to be estimated. Nevertheless, eqn. (3) and (4) offer important information about the ideal sampling distribution. By eqns. (4) it is also seen that the coefficient of variation of the estimate of the failure probability is proportional to $N^{-1/2}$.

At present more than forty different papers on importance sampling techniques are known to the authors (for a review see Melchers [7]) covering about ten different schemes, some of which differ only in details and implementation. It appeared appropriate to distinguish between

- Direct methods
- Updating methods
- Adaptive schemes
- Spherical schemes

which are briefly reviewed.

3.2. Direct methods

By the direct methods (also called static or nonadaptive methods) an important region is found or preselected and the sampling density is centered in this region. The earliest proposal for a sampling density is the uniform density [2]. But this choice does not lead to an unbiased probability estimate. The sampling density can also be the original density centered on the failure boundary [8]. The n-dimensional normal distribution with the same covariance matrix as f_X centered in the retransformed design-point has also been suggested [9,10]. Melchers [11] suggests to use the n-dimensional normal distribution centered in the point of maximum likelihood on the failure boundary with covariance not less than those of the respective X_i. Fujita and Rackwitz [3] performed the simulation in the u-space and used an n-dimensional standard normal distribution with independent components centered in the design point. The sampling density can also be constructed by excluding a part of the safe region [12,13].

The advantage of these methods as compared with simple Monte Carlo simulation is evident. If the failure function is not extremely nonlinear, about one half of the simulations falls in the failure region. Given that the important region can be located, the method is not sensitive towards the existence of multiple β-points, because a wide region is included in the sampling space [11]. Another important advantage of the direct methods is that the sampling can be carried out in the x-space. These methods all depend on some search algorithm to locate the important region. If the search fails, the method fails. Gradient based algorithms imply that g and F_X have to be continuous. The number of g-function calls which are necessary to perform N simulations is

$$N_g = K_1(n+1) + N \tag{5}$$

where K_1 is the number of iterations necessary to locate the important region.

A less intuitive approach is taken by Maes et al. [14] based on results of Breitung [5]. They construct a sampling density which approaches the ideal sampling density (see eqn. (4)) as p_f approaches zero. A new coordinate system (y) is introduced with origin at the point of maximum likelihood on the limit state surface and the first coordinate pointing towards the direction of steepest descent of the state function and the other towards the direction of the

principal curvatures. Let $L = \ln f_X(\boldsymbol{x})$ denote the log-likelihood function of Y and let the point of maximum likelihood be such that the matrix

$$\boldsymbol{W} = \left\{ \left[\frac{\partial^2 L}{\partial y_i \partial y_j} - \frac{\left|\frac{\partial L}{\partial y}\right|}{\left|\frac{\partial g}{\partial y}\right|} \frac{\partial^2 g}{\partial y_i \partial y_j} \right]_{i,j=2,\ldots,n} \right\} \tag{6}$$

has non-zero determinant. Then the first variable is stochastically independent from the other $(n-1)$ variables and has approximately an exponentially distribution with mean $1/|\nabla L|$. The remaining $(n-1)$ variables have a multivariate normal density with zero mean and covariance matrix $\boldsymbol{W}^{-1}$. This distribution is used as the importance sampling density. For each simulation it is necessary to perform the transformation from x- to y-space. This is a simple linear transformation.

For this method the computational effort increases rapidly with space dimension because it is necessary to determine the Hessian matrix of the failure surface in the point of maximum likelihood at least via a difference scheme. The total number of g-function calls is

$$N_g = K_1(n+1) + n(n-1)/2 + K_2 N \tag{8}$$

where $K_2 \geqslant 1$ is the number of g-function calls necessary for each simulation.

3.3. Updating method

An updating method has been suggested by Hohenbichler and Rackwitz [15], setting out from a SORM analysis but FORM can also be used as a basis. The basic variables are transformed into independent, standard normal variables $\boldsymbol{U}$ and an estimate for the failure probability is calculated as

$$\hat{p}_f = P(A)\frac{P(\Omega_f)}{P(A)} = P(A)C \tag{9}$$

where $P(A)$ is the approximate failure probability calculated by FORM or SORM. Sampling is carried out on the tangent to the failure surface in the most likely failure point and the correction factor, for example for a FORM analysis, is

$$C = \frac{P(\Omega_f)}{P(A)} = \frac{1}{N}\sum_{i=1}^{N} \frac{\Phi(-|\boldsymbol{u}^* + b_i\boldsymbol{\alpha}|)}{\Phi(-\beta)} \tag{10}$$

where $\boldsymbol{u}^*$ is the most likely failure point, β the geometrical reliability index, $\boldsymbol{\alpha}$ the unit vector of $\boldsymbol{u}^*$ and b_i is the root of $g(\boldsymbol{u}_i + b_i\boldsymbol{\alpha}) = 0$. For the FORM analysis the sampling density is the standard normal density. A quite similar approach is used when updating a SORM estimate. In that case the covariance of the sampling density is adjusted to the curvature of the failure surface in the most likely failure point. This concept has been extended to intersections of failure domains by Schall et al. [16] where the covariance of the sampling density is made dependent on a representative angle between the limit state functions.

The estimate eqn. (10) should have small variance because part of the integral is evaluated analytically. In this method an x- to u-space transformation is necessary for each g-function

call and g and F_X have to be continuous. It is further necessary to perform a line search in order to solve the equation $g(\boldsymbol{u}_i + b_i\boldsymbol{\alpha}_i) = 0$. When updating a FORM estimate the number of g-function calls is

$$N_g = K_1(n+1) + K_3 N \tag{11}$$

where $K_3 \geqslant 1$ is the number of g-function calls in the mentioned line search (usually 4–6). If the evaluation of $P(A)$ is based on a SORM analysis additional g-function calls are necessary in order to determine the curvatures of the limit state function in the design point but the line searches require somewhat smaller effort. The number of g-function calls becomes

$$N_g = K_1(n+1) + n(n-1)/2 + K_3 N \tag{12}$$

3.4. Adaptive sampling

Adaptive sampling is based on the idea that the knowledge about the failure domain increases as the number of simulations increases. At first the initial sampling density, an n-dimensional normal density [17,18] or a density with the same form as the original [19], is centered in a point of the failure region. A number of simulations are performed and the sampling density is updated before a new set of simulations is carried out. Wu [20] suggests a scheme where the sampling domain is varied incrementally by changing the curvatures of parabolic approximations of the failure surface in the most likely points of failure. The efficiency of the adaptive methods depends to a large extent on the initial guess of the important region. If the guess is bad, the method is not efficient. The starting point is often determined by pre-sampling [17,21]. The total number of g-function calls is

$$N_g = N^* + N \tag{13}$$

where N^* is the number of pre-samplings. For this method continuity of $F_X(\boldsymbol{x})$ and differentiability of $g(\boldsymbol{x})$ are not required and its implementation can be done in either x- or u-space.

3.5. Spherical sampling

Let the region Ω_f be such that every line starting at origin has only one intersection with the failure surface then eqn. (2) can be written as:

$$p_f = \int_{\Omega_f} \frac{f_X(\boldsymbol{v})}{h_V(\boldsymbol{v})} h_V(\boldsymbol{v})\, \mathrm{d}\boldsymbol{v} = \int_{\substack{\text{unit}\\ \text{sphere}}} \left[\int_{r(\boldsymbol{a})}^{\infty} \frac{f_X(s\boldsymbol{a})}{h_V(s\boldsymbol{a})} f_R(s|\boldsymbol{a})\, \mathrm{d}s \right] f_A(\boldsymbol{a})\, \mathrm{d}\boldsymbol{a} \tag{14}$$

where $\boldsymbol{a}$ is a unit direction vector and $r(\boldsymbol{a})$ is the distance to the region Ω_f in the direction $\boldsymbol{a}$. $f_R(s\,|\,\boldsymbol{a})$ is the density function of R given $A = \boldsymbol{a}$, where R and $\boldsymbol{A}$ are given by:

$$V = RA \tag{15}$$

The spherical sampling can be performed in both x- and u-space (see Ditlevsen et al. [22]). However, if the simulation is performed in the x-space, the integration in the direction $\boldsymbol{a}$ has to be performed numerically. As sampling densities Ditlevsen, Melchers and Gluver [22] suggest

to use $\mathscr{D}$-truncated μ-centered standard Gaussian distributions where μ is a position vector and $\mathscr{D}$ a subset of $\mathbb{R}^n$.

As for the updating method a contribution to $\hat{p}_f$ is obtained for each finite value of $r(\boldsymbol{a})$. The efficiency is, nevertheless, expected to depend on the number of variables. For larger number of variables a larger number of important directions exists. Several g-function calls for each simulation are necessary in order to solve the equation $g(r\boldsymbol{a}) = 0$. The total number of g-function calls is

$$N_g = K_1(n+1) + K_3 N \tag{17}$$

In this case the number $K_3 \geqslant 1$ must be expected to be slightly larger than for the updating method because less good initial values for the line searches are available.

4. Discussion of results

Seventeen inquiries were sent out in autumn 1991 to inventors of importance sampling schemes. In the questionnaire 10 examples covering a wide range of applications were included six of which are discussed in some detail below. About one third of these inventors supplied sufficiently complete answers analyses. They well represent the above mentioned different lines of approach.

Method A1 The direct method where a gaussian distribution with the same covariance matrix as f_X is used as the sampling density [9–11].
Method A2 Same as A1 but the covariance matrix is multiplied with a factor.
Method B The asymptotic method according to Maes et al. [14].
Method C The updating method based on a FORM estimate [15].
Method D The asymptotic updating method based on a SORM estimate [15].
Method E Spherical sampling [22,23].

For all examples the participants of the benchmark study were asked to determine the number of g-function calls necessary to reach a coefficient of variation of $V(\hat{p}_f) = 0.10$. However, not all participants have answered this question. The comparison of the efficiency of the methods, therefore, in part has to be based on an estimate of the number of g-function calls. The number can be estimated because it is known that the coefficient of variation is a linear function of $N^{-1/2}$ and it is known how N depends on the number of g-function calls (the K_i's are known).

Except for the adaptive sampling method a suitable algorithm must have first located the most likely failure point although in many of the examples this point could have been determined analytically. All the methods represented in this study use a gradient-based search algorithm to locate the important region. f_X and g have to be continuous. In order to allow for a fair comparison of the numerical effort it was assumed that the location of the most likely failure point required $4(n+1)$ g-function calls throughout. All methods locate the important region iteratively. It was suggested that the participants start their algorithm and the selection procedure for the sampling density with least possible knowledge about the problem. Unfortunately not all participants followed this suggestion. In fact, one can state that the participants tried to make the best out of their method. In practical applications where this prior knowledge usually is not available one or the other method must be expected to be considerably less efficient than indicated in this study. In the following the most important results are presented.

5. Examples

The examples are summarized in Table 1 for easy reference. Also the exact solutions are given. The examples thus can be used as a set of standard tests for evaluating the performance of an importance sampling method.

TABLE 1

Examples (N: Normal distribution, LN: Lognormal distribution, EXI: Gumbel distribution, EXP: Exponential distribution)

No	Limit state function	Purpose	Ref.
1	$g_1 = \beta n^{1/2} - \Sigma_{i=1}^{n} U_i$ $U_i \sim$ N(0, 1) $n = 2,\ n = 10,\ n = 50$ $\beta = 1.0,\ \beta = 5.0,\ \beta = 10.0$ $P_f = 0.159,\ 2.92 \cdot 10^{-7},\ 8.154 \cdot 10^{-24}$	Number of variables, Probability level	
2	$g_2 = \pm \Sigma_{i=1}^{n} X_i \mp C$ $X_i \sim$ EXP(λ) $C = 25.900,\ 31.856,\ 36.720,$ $41.050,\ 45.067,\ 48.932$ $-C = 14.525,\ 11.077,\ 8.951,$ $7.435,\ 6.277,\ 5.343$ $P_f = 10^{-1},\ 10^{-2},\ 10^{-3},\ 10^{-4},\ 10^{-5},\ 10^{-6}$	Nonlinearity Probability level	[3]
3	$g_4 = X_1 X_2 - PL$ $X_1 \sim$ N(78064.4, 11709.7) $X_2 \sim$ N(0.0104, $1.56 \cdot 10^{-3}$) $P = 14.614, \quad L = 10.0$ $P_f = 1.451 \cdot 10^{-6}$	Multiple β-points	[24]
4	$g_6 = \min(g_{61}, g_{62}, g_{63})$ $g_{61} = X_1 + 2X_3 + 2X_4 + X_5 - 5X_6 - 5X_7$ $g_{62} = X_1 + 2X_2 + X_4 + X_5 - 5X_6$ $g_{63} = X_2 + 2X_3 + X_4 - 5X_7$ $X_1 = X_2 = X_3 = X_4 \sim$ LN(60, 6.0) $X_6 \sim$ EXI(20, 6.0), $\quad X_7 \sim$ EXI(25, 7.5) $P_f = 2.0 \cdot 10^{-2}$	Series system	[11]
5	$g_8 = \max(\beta_i - \gamma_i^T U)$ $U \sim$ N(0, 1) $\beta_i = 2.5 + 0.25 \cos(\pi i / n)$ $\gamma_{ij} = 1$ for $j = i$ and $j = i+1$, 0 else $P_f = 2.087 \cdot 10^{-4}$	Parallel system system	[23]
6	$g_{10} = X_1 + 2X_2 + 2X_3 + X_4 - 5X_5 - 5X_6$ $+ 0.001 \Sigma_{i=1}^{6} \sin(100 X_i)$ $X_1 = X_2 = X_3 = X_4 \sim$ LN(120, 12) $X_5 \sim$ LN(50, 15), $\quad X_6 \sim$ LN(40, 12) $P_f = 1.23 \cdot 10^{-2}$	Noisy limit state function	[6]

5.1. Example 1

The first example is a n-dimensional hyperplane:

$$g_1 = \beta n^{1/2} - \sum_{i=1}^{n} U_i \tag{17}$$

where U_i, $i = 1, 2, \ldots, n$ are independent standard normal distributed variables. The example was to be calculated for $\beta = 1.0$, $\beta = 5.0$ and $\beta = 10.0$ for $n = 2$, $n = 10$ and $n = 50$. Its purpose is to check the random number generator and to investigate the performance of the methods for different probability levels and different numbers of stochastic variables.

In Fig. 1(a) the estimates of the failure probability relative to the exact value are shown as a function of the number of simulations, N (for $n = 10$ and $\beta = 5.0$). The coefficients of variations of these estimates are shown in Fig. 1(b). Since the limit state function is linear, the updating methods (method C and D) determine the exact failure probability and the coefficient of variation is zero. The random number generator cannot be judged by this example. However, extensive previous testing has proven the fitness of the generator used for method C and D. For all other methods a good estimate of the failure probability is obtained for $N = 5000$ (see Fig. 1(a)), and the coefficient of variation becomes smaller as the number of simulations increases (see Fig. 1(b)). The other investigated combinations of n and β show essentially the same behavior. It is concluded, that the random number generators implemented by the participants are all sufficiently good.

In Fig. 2(a) the coefficient of variation of the failure probability estimate is shown for $\beta = 5.0$ and $N = 500$ for different numbers of stochastic variables, n. Method C and D have zero coefficient of variation. The spherical sampling (method E) has been conducted with a standard n-dimensional normal distribution centered in the design point. The accuracy therefore decreases as the number of dimensions increases, because a larger number of important

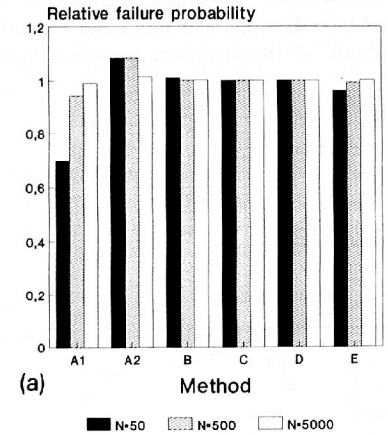

Fig. 1(a). Relative failure probability, example 1 ($n = 10$, $\beta = 5.0$).

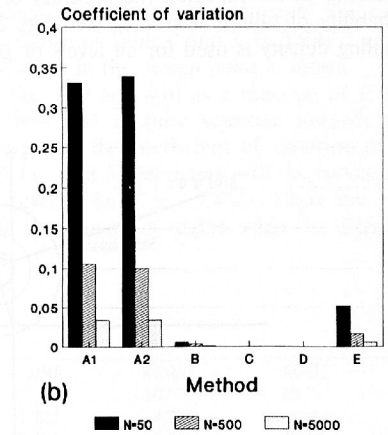

Fig. 1(b). Accuracy, example 1 ($n = 10$, $\beta = 5.0$).

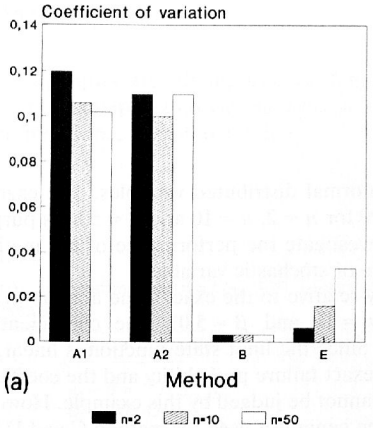

Fig. 2(a). Sensitivity towards dimension ($\beta = 5.0$, $N = 500$).

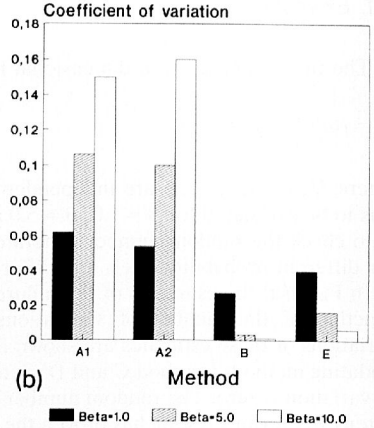

Fig. 2(b). Sensitivity towards reliability level ($n = 10$, $N = 500$).

directions exists. For all other methods the number of dimensions seems to have little or no effect on the coefficient of variation.

Figure 2(b) shows, the coefficients of variation for $n = 10$ and $N = 500$ for different values of β. The accuracy of the direct methods (methods A1 and A2) decreases as β increases (see Fig. 2(b)). As β increases the volume of the region around the design point which gives a significant contribution to p_f decreases (the marked region in Fig. 3). Because the standard deviation of the sampling density is independent of β fewer samples fall in the region which gives a significant contribution to p_f as β increases. The variance of $\hat{p}_f$ therefore becomes larger with increasing β. As expected the accuracy of method B (asymptotic sampling) increases as the probability of failure decreases (see Fig. 2(b)). In method E (spherical sampling) the same sampling density is used for all levels of β. The "spread" of the directions becomes smaller

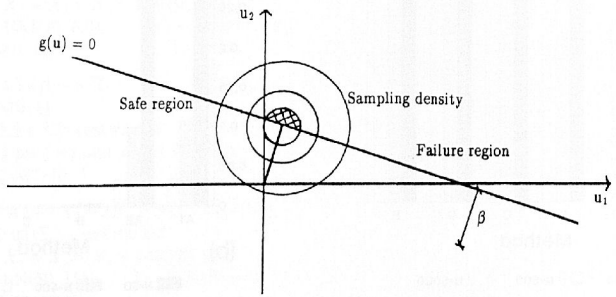

Fig. 3. Limit state surface for $n = 2$.

TABLE 2

Example 2, negative curvatures

$-C$	16.175	11.077	8.951	7.435	6.277	5.343
P_f	0.20	10^{-2}	10^{-3}	10^{-4}	10^{-5}	10^{-6}
β	0.841	2.328	3.093	3.722	4.268	4.765
r_i	−5.964	−5.139	−4.748	−4.444	−4.194	−3.976

with larger values of β. A larger number of the simulations then falls in the most important directions, and the variance of $\hat{p}_f$ becomes smaller as β increases (see Fig. 2(b)).

In this example the same covariance matrix has been used by method A1 and A2 (the covariance matrix for method A2 has been multiplied with a factor 1.0). It is seen, that approximately the same coefficients of variation of the failure probability estimates are obtained (see Figs. 1(a), 2(a) and 2(b)). The small differences can be ascribed to differences between the random number generators and computer implementation.

5.2. Example 2

The limit state function in the second example is

$$g_2 = \pm \sum_{i=1}^{n} X_i \mp C \tag{19}$$

where X_i, $i = 1, 2, \ldots, n$ are independent and exponentially distributed with the parameter λ [3]. The limit state function becomes highly non-linear in the u-space

$$g_2 = \pm \sum_{i=1}^{n} \ln[\Phi(-U_i)]/\lambda \pm C \tag{20}$$

where U_i are independent and normally distributed, $i = 1, 2, \ldots, n$. The exact probability of failure is $F_{Ga}(C; n; \lambda)$, where F_{Ga} denotes the gamma distribution. The example has been calculated for $\lambda = 1.0$ and $n = 20$ for the values of C shown in Table 2 and 3. In Table 2 and 3 also the radius of the curvatures of the limit state function in the design point is shown.

The coefficients of variation of $\hat{p}_f$ are shown in Fig. 4(a) and 4(b) as a function of C for $N = 500$. The accuracy of the direct method (method A1) is quite sensitive towards the curvature of the failure boundary. For negative curvatures the coefficient of variation of $\hat{p}_f$ increases with decreasing values of $-C$ (see fig. 4(a)), i.e. Var($\hat{p}_f$) increases with the curvatures and the distance between origin and design point (except for $C = -7.435$). There are two reasons for this behavior. First fewer samples fall in the important region when the distance

TABLE 3

Example 2, positive curvatures

C	25.900	31.856	36.720	41.050	45.067	48.932
P_f	10^{-1}	10^{-2}	10^{-3}	10^{-4}	10^{-5}	10^{-6}
β	1.282	2.328	3.093	3.722	4.268	4.765
r_i	7.725	7.975	8.506	8.954	9.351	9.720

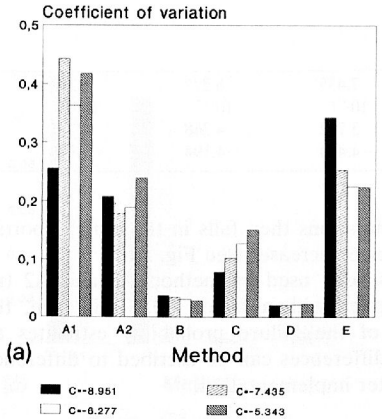

Fig. 4(a). Negative curvatures, Example 2.

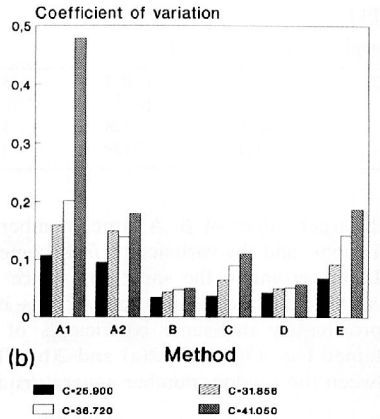

Fig. 4(b). Positive curvatures, Example 2.

between design point and origin increases, and secondly the important region becomes smaller as the curvature increases and thereby fewer samples fall into the failure region. For positive curvatures the coefficient of variation decreases as the curvature increases and the probability of failure decreases (for decreasing values of C) because this implies that a larger number of samples fall in the important region.

For negative curvatures of the limit state function, the results obtained by method A2 are based on a covariance matrix of the sampling density which is a factor 0.88 smaller than by method A1. For negative curvatures only a small region around the design point gives a contribution to p_f and therefore method A2 yields better results than method A1 (see Fig. 4(a)). For positive curvatures, the sampling has been conducted with a covariance matrix of the sampling density which is a factor 1.2 larger than by method A1. For positive curvatures of the limit state function, a significant contribution to p_f comes from regions away from the design point. This leads to better results than by method A1 (see Fig. 4(b)). Method A2 seems to be less sensitive towards the curvatures of the limit state function than method A1.

For method B the accuracy of $\hat{p}_f$ increases as the failure probability decreases and the negative curvatures increase (see Fig. 4(a)). This can be explained by the fact that the sampling density improves as p_f decreases (see also example 1). It should be expected that as p_f decreases and the positive curvatures decrease the coefficient of variation of $\hat{p}_f$ decreases because a better approximation to the ideal sampling density is obtained and less samples fall in the safe region. This is, however, not the case (see Fig. 4(b)). For lower reliabilities and positive curvatures a larger number of samples fall into unimportant regions which causes a decrease of the accuracy.

For method C the sampling density is independent of the reliability level and the curvature of the failure surface in the design point. This means that for low reliability levels a large number of simulations fall in unimportant regions. The coefficient of variation of the failure probability estimate thereby increases for decreasing p_f (see Figs. 4(a) and 4(b)). For positive curvatures, the important region is considerably larger than for negative curvatures. Therefore, the accuracy is generally better for positive curvatures (see Fig. 4(a) and 4(b)).

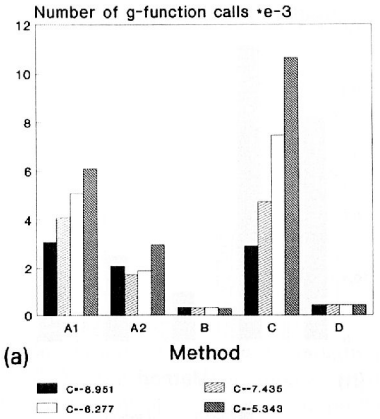

Fig. 5(a). Efficiency, negative curvatures, Example 2.

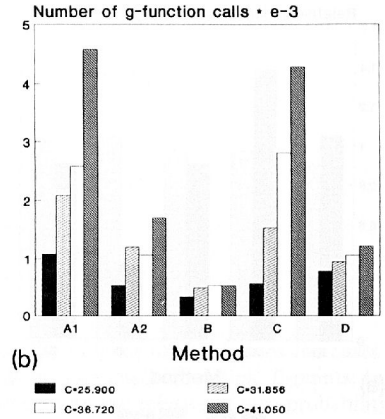

Fig. 5(b). Efficiency, Positive curvatures, Example 2.

In Fig. 4(a) and 4(b) it is seen that for method D the coefficient of variation of the failure probability slightly increases with decreasing probability level, independent of the curvature of the failure surface. This can be explained by the fact that the variance of the sampling density, which is adjusted to the curvatures in the design point, does not depend on the probability level. This causes the coefficient of variation to increase when the probability level decreases because a larger number of the simulations falls into unimportant regions.

The spherical sampling has been performed with a standard normal density centered at the design point. For method E the variance of $\hat{p}_f$ is large for negative curvatures because only a small number of the samples intersect with the failure surface (see Fig. 4(a)). As could be expected the accuracy decreases with increasing negative curvatures. If the curvatures are positive a large number of simulations are successful. The accuracy thereby increases with increasing positive curvatures (see Fig. 4(b)).

In Fig. 5(a) and 5(b) the number of g-function calls necessary to obtain a coefficient of variation, $V = 0.10$ is shown for the different methods. Figure 5(a) and 5(b) does not lead to any new conclusions about the sensitivity of the methods towards the curvature of the failure surface or probability level. The most efficient methods are methods B and D. It is interesting to notice that even though method C achieves a much better accuracy than method A for the same number of simulations (see Figures 4(a) and 4(b)), method C may require more g-function calls. For method E (not shown in Figs. 5(a) and 5(b)) the number of simulations to achieve C.O.$V(\hat{p}_f) = 0.1$ for negative curvatures is in the order of 2000–3000. Since for each simulation a number of g-function calls are necessary in order to perform a line search the total number of g-function calls becomes rather large.

5.3. Example 3

In example 4 the limit state function is a hyperbola [24]:

$$g_4 = X_1 X_2 - PL \tag{21}$$

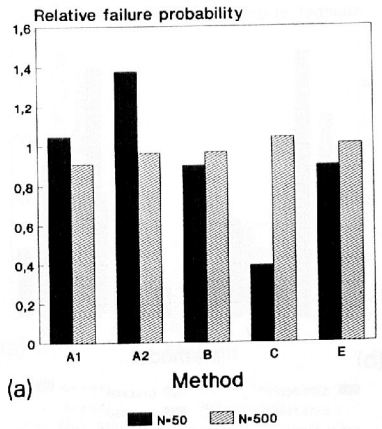

Fig. 6(a). Relative failure probability, Example 4.

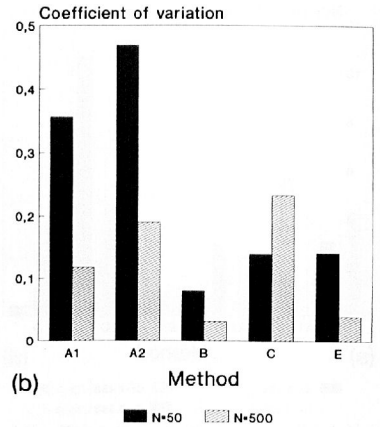

Fig. 6(b). Accuracy, Example 4.

where P and L are deterministic parameters with values, 14.614 and 10.0, respectively. X_1 and X_2 are normally distributed variables with means, 78064.4 and 0.0104, and standard deviations, 11709.7 and 0.00156, respectively. The example serves to evaluate the robustness of the methods with respect to multiple β-points. Here two minimum points and one maximum point exist.

In Fig. 6(a) the estimates of the failure probability relative to the exact solution are shown for $N = 50$ and $N = 500$. The coefficients of variation of $\hat{p}_f$ are shown in Fig. 6(b). The "exact" failure probability, $p_f = 1.451 \cdot 10^{-6}$ has been determined by conditional integration [24].

For method A1 the coefficient of variation should decrease rather steadily as the number of simulations increases and for $N = 500$ a good estimate of the failure probability is obtained (see Figs. 6(a) and 6(b)). Because the sampling density covers a large area the method is not sensitive towards the existence of multiple β-points. The results for method A2 has been obtained on the basis of a sampling density with a smaller covariance matrix by a factor 0.8. The spread of the samples then becomes smaller and the coefficient of variation of the failure probability estimate larger (see Fig. 6(b)). Method B appears to yield very good results for this example. The sampling, however, has been performed with a stratified sampling density (see example 4 for further explanation) and it is therefore not possibly to judge if the method is sensitive towards the existence of multiple β-points.

For method C the sampling density is centered in the design point which is determined when the search-algorithm is started in the mean value point. This point lies on the symmetry axis (see Fig. 7) and is, in fact, no valid β-point. This implies that in the area around the two other β-points the relation f_X/h_Y becomes large whereby the coefficient of variation also becomes large (see eqn. (4)). The results (see Figs. 6(a) and 6(b)) show that for $N = 50$ the estimate of the failure probability is biased and simultaneously the coefficient of variation is small. This indicates that for $N = 50$ only few simulations have fallen in the vicinity of the two other β-points. For $N = 500$ sufficiently many simulations fell in the important regions and the failure probability estimate is satisfactory, although with rather high coefficient of variation. The fact

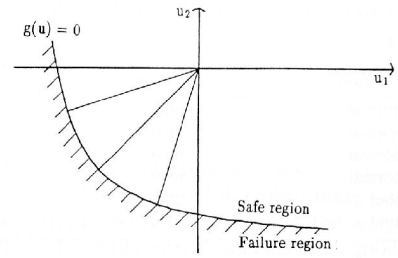

Fig. 7. Limit state surface, Example 4.

that the coefficient of variation actually increases as the number of simulations increases (see Fig. 6(b)) proves that this method is sensitive towards the existence of multiple β-points. In Fig. 8 the coefficient of variation of the probability estimate and the relative failure probability are shown as functions of the number of simulations. The jumps in the curves denote simulations where an important region was hit. The general appearance of this figure also holds for the majority of the other methods. Moreover, one can conclude that only a careful monitoring of the coefficient of variation function can indicate the presence of multiple β-points, but only if the sampling distribution is not too narrow. The example has not been calculated by method D because a SORM analysis would have failed without prior knowledge about the actual shape of the failure function.

The spherical sampling (method E) is conducted in the u-space and the sampling density is standard gaussian centered at the origin. In Fig. 6(a) and 6(b) it is seen that $\hat{p}_f$ approaches the exact value as the number of simulations increases, and that the coefficient of variation of the estimate is small. The method is very efficient since the number of dimensions is small. The example has also been calculated with a sampling density located at one of the two most central points (see Fig. 7). Also in that case the probability estimate rapidly approaches the exact value. The coefficient of variation, however, is larger. The method, therefore, must also be viewed as sensitive towards the existence of multiple β-points.

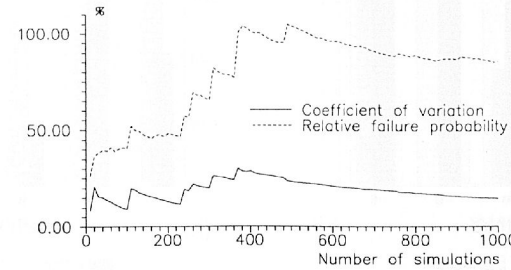

Fig. 8. Coefficient of variation for method C.

TABLE 4

Stochastic variables for example 4

Variable	Distribution	Mean	Stand. dev.
X_1	Lognormal	60.0	6.0
X_2	Lognormal	60.0	6.0
X_3	Lognormal	60.0	6.0
X_4	Lognormal	60.0	6.0
X_5	Gumbel	20.0	6.0
X_6	Gumbel	25.0	7.5

5.4. Example 4

Example 4 is a series system [11,25]. The failure functions are:

$$\left.\begin{aligned} g_{61} &= X_1 + 2X_2 + 2X_4 + X_5 - 5X \\ g_{62} &= X_1 + 2X_2 + X_4 + X_5 - 5X_6 \\ g_{63} &= X_2 + 2X_3 + X_4 - 5X_6 \end{aligned}\right\} \tag{22}$$

All variables are independent and the parameters are given in Table 4. The purpose of this example is to test whether the methods can handle series systems. The estimates of the failure probability relative to the "exact" failure probability are shown in Fig. 9(a) and the coefficients of variation in Fig. 9(b). The "exact" $p_f = 2.0 \cdot 10^{-2}$ is calculated by direct Monte Carlo simulation [25]. Simulations can be carried out without problems for each of the three limit state functions since none of the failure surfaces contains multiple β-points and none is highly

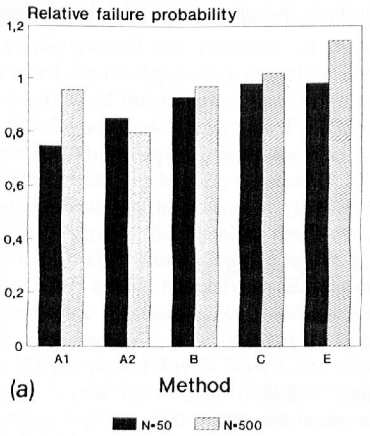

Fig. 9(a). Relative failure probability, Example 6.

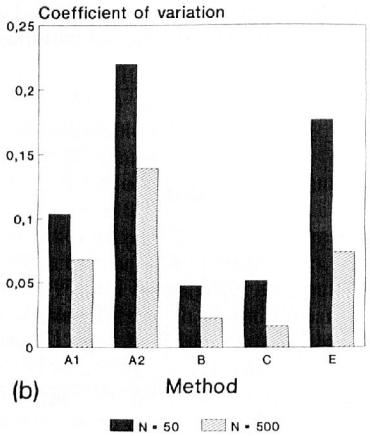

Fig. 9(b). Accuracy, Example 6.

nonlinear. All the investigated methods deal with series systems by introducing a stratified sampling density:

$$h_V(v) = \sum_{i=1}^{m} w_i h_{V_i}(v)$$

where m indicates the number of limit state functions and w_i is a weight factor. The weight factors are chosen such that $w_i > 0$ and $\sum_{i=1}^{m} w_i = 1.0$. Unfortunately, it is not quite obvious from the reported results how the various methods introduced the weights for the different limit state functions. All methods can handle series systems and good estimates of the failure probability are obtained (see Fig. 9(a)). The best estimates and the smallest coefficients of variation are obtained by methods B and C.

5.5. Example 5

Example 8 is a parallel system with four limit state functions:

$$\left.\begin{aligned} g_{81} &= 2.677 - U_1 - U_2 \\ g_{82} &= 2.500 - U_2 - U_3 \\ g_{83} &= 2.323 - U_3 - U_4 \\ g_{84} &= 2.250 - U_4 - U_5 \end{aligned}\right\} \tag{23}$$

where U_i, $i = 1, 2, \ldots, 5$ are independent standard normally distributed variables. The purpose of the example is to check whether the methods can handle parallel systems. The coefficients of variation of the estimates of the failure probability and the failure probability estimates relative

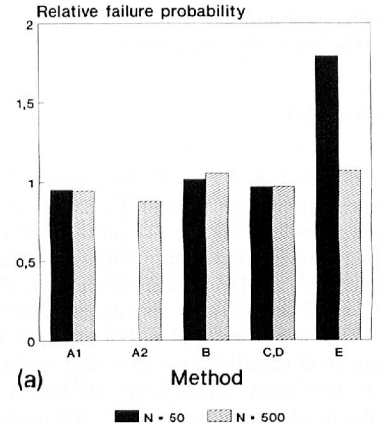

Fig. 10(a). Relative failure probability, Example 8.

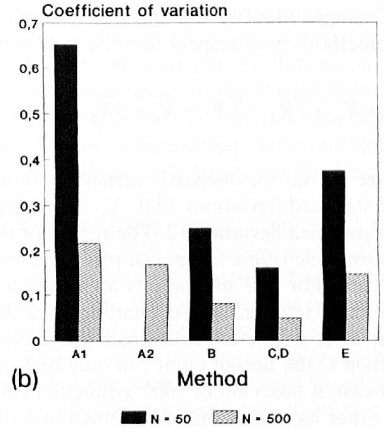

Fig. 10(b). Accuracy, Example 8.

to the exact solution are shown in Fig. 10(b) and 10(a) respectively. The exact failure probability, $p_f = 2.087 \cdot 10^{-4}$, is determined by a FORM analysis, where the limit state functions are linearized in the joint design point. In Fig. 10(a) it is seen that all methods can handle parallel systems and that for $N = 500$ good estimates of p_f are obtained.

The coefficient of variation which has been obtained by the direct method (Method A1) is much larger than in example 1 under similar circumstances (the same distance to the design point and the same number of variables). This can be explained by the fact that in example 1 about half of the simulations fell into the failure region. For this example only about 1/16 of the simulations fall in the failure region. The coefficient of variation therefore becomes larger (see eqn. (4)). The accuracy obtained by method A2 is better than for method A1 because the covariance matrix of the sampling density has been multiplied with a factor 0.8, whereby a larger number of samples falls in the region around the design point.

For this example the accuracy of the failure probability estimate for method B is considerably larger than for the other examples (see Fig. 10(b). This indicates that the asymptotic sampling density fails to provide a good fit to the ideal sampling density.

The updating method (method C and D) is very efficient (see Fig. 10(b)) because the spread of the sampling density is adjusted to the angle between the tangents of the failure surfaces in the design point (see Schall et al. [16]). Most of the simulations therefore give a relatively large contribution of $\hat{p}_f$.

The result of spherical sampling is based on stratified sampling density: the standard normal distribution centered at origin and a simplex truncated normal distribution, respectively. The simplex corresponds to all variables being non-negative. The weight factors are 0.2 and 0.8. Because the angle between the failure surfaces is relatively small only few of the samples gives a contribution to p_f. The coefficient of variation of the estimate of the failure probability is relatively high (see Fig. 10(b)).

5.6. Example 6

Example 10 (after Liu and Der Kiureghian [6]) was included in order to test the efficiency of the methods with respect to noisy failure boundaries. The limit state function is:

$$g_{10} = X_1 + 2X_2 + 2X_3 + X_4 - 5X_5 - 5X_6 + 0.001 \sum_{i=1}^{6} \sin(100X_i) \tag{24}$$

where all the six stochastic variables are log normally distributed. X_1 to X_4 have means 120. and standard deviations 12.0. X_5 has mean 50 and standard deviation 15, and X_6 has mean 40 and standard deviation 12. The results of the example are shown in Fig. 11. For all the methods this example offers no special problems for the sampling schemes once the important region is selected. For 500 simulations all methods achieve a coefficient of variation which is smaller than 0.10 (see Fig. 11). As mentioned earlier the efficiency of the methods also depends on the number of g-function calls which are necessary to locate the important region. For example, for method C the design point can only be located if a very good initial guess is provided. Even in that case it takes about 2000 g-function calls to find the most likely failure point. Method A on the other hand uses only 56 g-function calls to locate the important region. In this case method A clearly is the superior method. Method C and D (not shown) have constructed their sampling

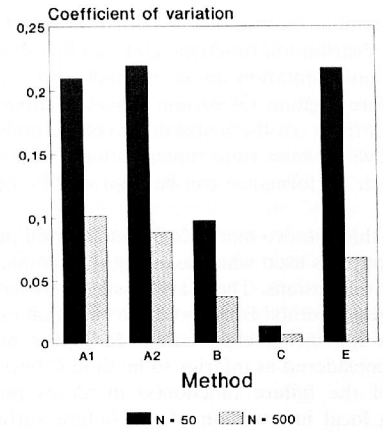

Fig. 11. Accuracy, Example 10.

densities by omitting the noisy term in eqn. (24). In this respect the results are of less significance for the purpose of this example.

6. Summary and conclusion

It is not possible to identify one of the methods as being the best under all circumstances. Three criteria appear to be most important when judging an importance sampling method:
- accuracy and efficiency
- sensitivity against number of variables
- sensitivity against multiple important regions and noisy limit state functions

Simple components and series systems with smooth failure functions and continuous distribution functions and not too high uncertainty spaces can be computed equally well by any method with approximately the same numerical effort. From the example calculations one may conclude that method A is always suitable if only moderate accuracy of the failure probability estimate is required. Higher accuracies require comparatively more effort. In this case methods C and E or even B and D should be used. Whenever the above mentioned ideal conditions do not hold remarkable differences between the various methods with regard to efficiency and robustness can be observed.

Methods B to E require precise knowledge of the most likely failure region(s). If this is known the efficiency of all these methods is acceptable and is, with the exception of method E, relatively insensitive to the space dimension. These methods fail or are inefficient whenever the most likely failure region(s) cannot be identified by one of the available gradient based search algorithms. Serious attempts to implement non-gradient based algorithms are not known but it must be expected that any search for the most likely failure region will then be very expensive. Part of the adaptive direct methods must just be viewed as one such non-gradient based search algorithm. Method C appears to be best suited for computing intersection probabilities even under extreme circumstances (very small cut sets).

The direct methods furthermore impose only weak requirements on the smoothness of the limit state functions and the distribution functions given an important region has been located. Depending on the specific implementation direct methods also appear to be relatively robust with respect to multiple failure regions. Of certain practical importance finally is the ease to implement a direct method in the x- or the u-space. Direct methods are on the other hand less efficient and can be ineffective for limit state functions with large curvatures. As indicated by the results of method A2 their performance can be improved by empirical adjustments to the sampling density.

It has been demonstrated that the two methods B and D based on asymptotic considerations and where curvature information is used when selecting the sample density are generally most efficient in spaces of smaller dimensions. There are small differences in efficiency between the methods with some advantage to method B. As both are based on essentially the same concepts the authors do not have a convincing explanation. In higher dimensions curvature based methods must, however, be considered as inferior to method C because the numerical effort to determine the Hessian(s) of the failure function(s) increases proportional to n^2. Because method B and D are using local information of the failure surface to adjust the sampling density these methods can, of course be especially misleading if a wrong important region is located. At a modified example 4 it can in fact be demonstrated that method B would exhibit very soon a very small coefficient of variation of the probability estimate for a wrong β-point thus giving the impression of high accuracy whereas the true probability is by more than one order of magnitude different.

The spherical sampling method E appears less suited for the analysis of problems in high dimensions. Moreover, it is sometimes difficult to select an appropriate sampling density when no detailed knowledge of the failure function is available.

Beyond those factors it is noticeable that not all methods have the same capabilities at least not in their present implementations. For example, from the available literature it appears that only methods C is able to handle equality constraints at present.

In Table 5 the authors have made an attempt to rate the different methods with respect to the different criteria on the basis of the reported results. The ratings are

- excellent: 10
- good: 7.5
- average: 5
- bad: 2.5
- unacceptable: 0

TABLE 5

Summary

	A	B	C	D	E
x-, u-space	10	10	5	5	7.5
Efficiency	5	10	7.5	10	5
Robustness	10	2.5	7.5	2.5	7.5
Capabilities	7.5	5	10	7.5	7.5
Insensitivity against curvatures	5	10	5	10	5
Insensitivity against dimension	5	5	7.5	5	2.5
Insensitivity against prop.level	7.5	10	7.5	10	5
Average	7.1	7.5	7.1	7.1	6.1

If such a rating is admissible at all in remembering that the merits and disadvantages of the various methods show up in different fields of application one can conclude that methods A to D are slightly preferable to method E. The differences are nevertheless small enough not to discriminate any of the methods. If the possibility of using an x-space formulation is not considered as advantageous method D is preferable to method B.

The selection of an importance sampling method for practical applications should be based on the available knowledge about the specific problem. If little is known method A is likely to be the most robust but not necessarily the most efficient. Method E as method A appear to be particularly suited for non-differentiable convex safe domains. If some smoothness requirements for the state and distribution functions are met method C or even one of the asymptotic methods (B or D) may be preferable. The final conclusion is this: In practical applications intelligent use of either concepts should be made and no prior preference for a particular method is justified which the authors admittedly had before this study.

Acknowledgements

This study would not have been possible without the ambitious help and cooperation of various groups which we highly appreciate. We would like to thank the following persons in alphabetical order for their contributions: O. Ditlevsen, A. Karamchandani, M.A. Maes, R. Melchers, M. Petschacher, J. Schneider, G.I. Schueller, R. Turner and Y.-T. Wu.

References

1 M. Hohenbichler, S. Gollwitzer, W. Kruse and R. Rackwitz, New light on first- and second-order reliability methods, *Structural Safety*, 4 (1987) 267–284.
2 M. Shinozuka, Basic analysis of structural safety, *J. of Struct. Eng.*, ASCE, 109 (1983) 721–740.
3 M. Fujita and R. Rackwitz, Updating first- and second-order reliability estimates by importance sampling, *Structural Eng. / Earthquake Eng.*, 5 (1988) 53–59.
4 R. Rackwitz and B. Fiessler, Structural reliability under combined random load sequences, *Comp. & Struc.*, 9 (1978) 484–494.
5 K. Breitung, Probability approximations for multinormal integrals, *J. of Eng. Mech.*, ASCE, 117 (1991) 457–478.
6 P.-L. Liu and A. Der Kiureghian, Optimization algorithms for structural reliability, *Structural Safety*, 9 (1991) 161–178.
7 R.E. Melchers, Simulation in time-invariant and time-variant reliability problems, Presented at the 4th IFIP WG7.5 Conference, Munich, 1991.
8 Y. Ibrahim, Observations of applications of importance sampling in structural reliability analysis, *Structural Safety*, 9 (1991) 269–281.
9 G. Fu and F. Moses, A sampling distribution for system reliability application, in: P.T.-Christensen (Ed.), *Proc. 1st IFIP WG 7.5 Working Conf. on Reliability and Optimization of Structural Systems*, Aalborg, May 6–8, 1987, Springer, Berlin, 1987.
10 G.I. Schueller and R. Stix, A critical appraisal of methods to determine failure probabilities, *Structural Safety*, 4 (1987) 293–309.
11 R.E. Melchers, Importance sampling in structural systems, *Structural Safety*, 6 (1989) 3–10.
12 R. Turner, Monte Carlo simulation methods of structural system reliability analysis, Brite Project P1271, Task III.3, 1991.
13 A. Harbitz, An efficient sampling method for probability of failure calculation, *Structural Safety*, 3 (1986) 109–116.

14 M.A. Maes, K. Breitung and D.J. Dupuis, Asymptotic importance sampling, Revised and re-submitted to Structural Safety, July 1992.
15 R. Hohenbichler and R. Rackwitz, Improvement of second-order reliability estimates by importance sampling, *J. of Eng. Mech.*, ASCE, 114 (1988) 2195–2199.
16 G. Schall, Z. Gollwitzer and R. Rackwitz, Integration of multinormal densities on surfaces, reliability and optimization of structural systems '88, in: P.T.-Christensen (Ed.), *Proceedings of the 2nd IFIP WG7.5 Conference*, London, UK, Springer Verlag, 1988, pp. 235–248.
17 C.G. Bucher, Adaptive sampling—an iterative fast Monte Carlo procedure, *Structural Safety*, 5 (1988) 119–126.
18 R.E. Melchers, Search-based importance sampling, *Structural Safety*, 9 (1990) 117–128.
19 A. Karamchandani, P. Bjerager and C.A. Cornell, Adaptive importance sampling, in: A.H-S. Ang, M. Shinozuka, G.I. Schueller (Eds.), *Proceedings of the 5th ICOSSAR '89*, San Francisco, Vol. II, 1989, pp. 855–862.
20 Y.-T. Wu, An adaptive importance sampling method for structural system reliability analysis, to be presented at the ASME 1992 Annual Meeting, Symposium on Reliability Technology.
21 G.L. Ang, A.H.-S. Ang and W.H. Tang, Multi-dimensional kernel method in importance sampling, in: L. Esteva, S.E. Ruiz (Eds.) *Proc. 6th Int. Conf. on Applications of Statistics and Probability in Civil Engineering*, Mexico, 1991, 1, pp. 289–296.
22 O. Ditlevsen, R.E. Melchers and H. Gluver, General multi-dimensional probability integration by directional simulation, *Computers and Structures*, 36 (1990) 355–368.
23 P. Bjerager, Probability integration by directional simulation, *J. of Eng. Mech.*, ASCE, 114 (1988) 1285–1302.
24 U. Bourgund, Discussion to: Fujita, M., Rackwitz, R., Updating first- and second-order reliability estimates by importance sampling, *Structural Eng. / Earthquake Eng.*, 6 (1989) 201–203.
25 G.I. Schueller, C.G. Bucher, U. Bourgund and W. Ouypornprasert, On efficient computational schemes to calculate structural failure probabilities, *Probabilistic Engineering Mechanics*, 4 (1989) 10–18.

SUBMISSION OF PAPERS AND DISCUSSIONS

Papers and discussions should be submitted to the Editor, Professor Ross B. Corotis, Office of Engineering Dean, The Johns Hopkins University, Baltimore, MD 21218, USA, or to the Associate Editor, Professor Bruce R. Ellingwood, Department of Civil Engineering, The Johns Hopkins University, Baltimore, MD 21218, USA, or may be communicated through a member of the Editorial Board.

Submission of a manuscript implies that it is not under consideration for publication elsewhere and further that, with the exception of review papers, original work not previously published is being presented.

Three copies of the *manuscript* should be submitted in double-spaced typing on pages of uniform size with a wide margin on the left. The top copy should bear the name and full postal address of the person to whom proofs are to be sent. A summary of 100–200 words is required.

Submission of electronic text
In order to publish the paper as quickly as possible after acceptance, authors are encouraged to submit the final text also on a 3.5" or 5.25" diskette. Both double density (DD) and high density (HD) diskettes are acceptable. The diskette may be formatted with either MS-DOS/PC-DOS or with Macintosh OR. See the Notes for Electronic Text Preparation at the back of this issue for further information. The final manuscript may contain parts (e.g. formulae, complex tables) or last-minute corrections which are not included in the electronic text on the diskette; however, this should be clearly marked in an additional hardcopy of the manuscript. Authors are encouraged to ensure that apart from any such small last-minute corrections, **the disk version and the hardcopy must be identical**. Discrepancies can lead to proofs of the wrong version being made.

References should be numbered consecutively throughout the text and collected together in a reference list at the end of the paper. Journal titles should be abbreviated. The abbreviated title should be followed by volume number, year (in parentheses), and page number.

All *illustrations* and tables should be numbered consecutively and separately throughout the paper. Line drawings should be in a form suitable for reproduction, drawn in Indian ink on drawing paper. They should preferably all require the same degree of reduction, and should be submitted on paper of the same size as, or smaller than, the main text, to prevent damage in transit. Photographs should be submitted as clear black-and-white prints on glossy paper. Each illustration must be clearly numbered.

Legends to the illustrations must be submitted in a separate list.

The principal *language* of the journal is English.

Authors will receive *galley proofs*, which they are requested to correct and return as soon as possible. No new material may be inserted in the text at the time of proofreading.

A total of 50 *reprints* of each paper will be supplied free of charge to the author(s). Additional copies can be ordered at prices shown on the reprint order form which accompanies the galley proofs.

A pamphlet containing detailed instructions on the preparation of manuscripts for
STRUCTURAL SAFETY
may be obtained from the publishers.

0167-4730/93/$06.00

Printed in The Netherlands